Received: 5 January 2021 | Revised: 19 April 2021 | Accepted: 25 April 2021

DOI: 10.1002/aoc.6287

FULL PAPER

Applied Organometallic Chemistry WILEY

Cationic ruthenium(II)–NHC pincer complexes: Synthesis, characterisation and catalytic activity for transfer hydrogenation of ketones

Dibya Yadav | **Shilpi Misra** | **Dheeraj Kumar** | **Suryabhan Singh** | **Amrendra K. Singh**

Discipline of Chemistry, Indian Institute of Technology Indore, Indore, 453552, India

Correspondence
Amrendra K. Singh, Discipline of Chemistry, Indian Institute of Technology Indore, Indore 453552, India.
Email: aks@iiti.ac.in

Funding information
Science and Engineering Research Board, Grant/Award Number: EMR/2016/004076

Cationic ruthenium pincer complexes, [Ru(CNC)(CO)(PPh_3)Cl]X (CNC = 2,6-bis(1-methylimidazol-2-ylidene)-pyridine, X = Cl^- [**1a**], PF_6^- [**1b**]), [Ru(CNC)(PPh_3)$_2$Cl]X (X = Cl^- [**2a**], PF_6^- [**2b**]) and [Ru(CNC)(PPh_3)$_2$(H)]X (X = Cl^- [**3a**], PF_6^- [**3b**]) with triphenylphosphine, CO and halides as coligands have been synthesised and characterised by ^{1}H, ^{13}C, ^{31}P NMR, mass and single-crystal X-ray crystallography. The application of Ru complexes in the transfer hydrogenation of a wide range of ketones with 2-propanol as the hydrogen source is explored. The in situ transformations observed during the synthesis help understand and suggest a plausible mechanism via the hydride complex **3b**. All complexes appear to be efficient catalyst precursors for transfer hydrogenation of ketones.

KEYWORDS
catalysis, *N*-heterocyclic carbene, pincer ligand, Ru complex, transfer hydrogenation

1 | INTRODUCTION

Transition metal complexes with pincer type ligands have been investigated widely and used in numerous catalytic transformations.[1–9] The robust pincer ligand platform provides transition metal complexes with high thermal stability which have been applied to various catalytic reactions and small molecule activations, for example, dinitrogen activation,[10–13] labilisation of the N-H bonds in ammonia,[14,15] carbon dioxide reduction[16,17] and water splitting.[18–22] Among the variety of pincer ligands, pyridine–dicarbene pincer ligands with *N*-heterocyclic carbenes (CNC pincer ligands) have become increasingly popular ligands which increase the electron density at the coordinated metal and enhance the reactivity of the metal centre.[23]

There has been significant interest in ruthenium pincer complexes as catalysts due to being readily available in different stable oxidation states and different coordination geometries, namely, square pyramidal, trigonal-bipyramidal and octahedral.[1–4,9] Ru–CNC-type pincer complexes are widely reported in the literature with various coligands including halides, CO and phosphines.[24,25] Presence of different coligands on ruthenium centre can influence the electronic and steric properties and also allows interesting coordination chemistry. An important structural aspect of the complexes based on CNC pincer ligands is the type of wing-tip substituents on the *N*-heterocycle which are used to influence the steric environment around the central metal atom. CNC pincer ligands with bulky aromatic substituents on the *N*-heterocycles are the most common whereas examples with smaller alkyl substituents are somewhat less explored.

Hydrogenation/dehydrogenation reactions play a significant role in synthetic organic chemistry, and such reactions involving oxygenated compounds are particularly useful for manufacturing agrochemicals,

pharmaceuticals, foods and fuels.[26,27] Traditionally, these reactions have been carried out using high hydrogen pressure or a stoichiometric amount of hazardous reagents, various additives, and cocatalysts, which often produce copious waste.[27] On the other hand, transfer hydrogenation (TH) and acceptorless dehydrogenation are two of the most atom-efficient ways to access valuable intermediates and various organic transformations. Ruthenium-based complexes for TH of ketones and dehydrogenation of alcohols have been well studied.[1–4,26,27] Whereas Ru(II) complexes bearing pincer ligands have been well studied, complexes with CNC pincer ligands are less explored for the TH of ketones.[24,25] With an aim to utilise the robustness provided by the pyridine–dicarbene CNC pincer ligands while also allowing the freedom to have a variety of bulkier coligands, we have started investigating synthesis and reactivities of complexes with CNC pincer ligands having smaller alkyl substituents.

Herein, we report the synthesis, structure and catalytic activity of Ru(II)–CNC complexes, namely, [Ru(CNC)(CO)(PPh_3)Cl]X (X = Cl^- [**1a**], PF_6^- [**1b**]) and [Ru(CNC)(PPh_3)$_2$Cl]X (X = Cl^- [**2a**] and PF_6^- [**2b**]). A possible intermediate **3a/3b** was observed and also synthesised separately, which was supported by spectroscopic data. Further, the reactivities of complexes **1b**, **2b** and **3b** have been investigated for the TH of ketones, and the better performing catalyst precursor **1b** was used with a variety of ketones giving high conversions.

2 | EXPERIMENTAL

2.1 | General procedure

All reactions and manipulations were carried out under an inert atmosphere using the standard Schlenk technique. Solvents were purchased from S. D. Fine-Chem Limited and purified by distillation under an inert atmosphere. [RuHCl(CO)(PPh_3)$_3$][28] and [$RuCl_2$(PPh_3)$_3$][29] were prepared by following the literature procedure using $RuCl_3 \cdot 3H_2O$. Deuterated dimethyl sulphoxide was purchased either from EURISOtop or Aldrich Chemical Co. NMR spectra were taken on Bruker Avance (III) spectrometer operating at 400 (^{1}H), 162 (^{31}P) and 100 MHz (^{13}C). NMR chemical shifts are reported in ppm and referenced to the solvent peaks for ^{1}H (DMSO-d_6, δ 2.54 ppm) and ^{13}C (natural abundance of ^{13}C in DMSO-d_6, δ 40.45 ppm) NMR. ^{31}P NMR chemical shifts are referenced to an external 85% H_3PO_4 standard as 0 ppm. The mass chromatograms were recorded on Bruker-Daltonics-microTOF-QII mass spectrometer. Gas chromatography (GC) samples were analysed in Shimadzu QP2010 Ultra, without an internal standard.

2.2 | Synthesis of [Ru(CNC)(CO)(PPh_3)Cl]Cl, 1a

An oven-dried Schlenk tube with the magnetic stirring bar was charged with the ligand precursor **CNC·2HBr** (0.200 g, 0.5 mmol) and dried under vacuum at 100°C for 2 h. The Schlenk tube was cooled to room temperature under N_2 atmosphere. Dry methanol (10 ml) was added, followed by Ag_2O (0.116 g, 0.5 mmol) and stirred at room temperature in the dark, covered with aluminium foil. After 30 min, a white precipitate had formed, and [RuHCl(CO)(PPh_3)$_3$] (0.477 g, 0.5 mmol) was added to the reaction mixture. The reaction mixture was heated at 60°C for 24 h, which results in a brown colour solution with some residue. The reaction mixture was filtered through celite, and the filtrate was reduced in volume (2 ml) followed by the addition of diethyl ether (5 ml). The compound precipitated out as yellow solid. The X-ray quality crystals of **1a** with bromide as the halide ligand were obtained, at −18°C, by slow diffusion of diethyl ether in acetonitrile solution of the crude reaction mixture. Yield: 0.180 g (40%). ^{1}H NMR (400 MHz, DMSO-d_6, δ in ppm): δ 8.44 (d, J = 2.2 Hz, 2H), 8.11 (t, J = 8.1 Hz, 1H), 7.77 (d, J = 8.1 Hz, 2H), 7.56 (d, J = 2.2 Hz, 2H), 7.39–7.31 (m, 3H), 7.25 (td, J = 7.7, 2.1 Hz, 6H), 6.94 (dd, J = 10.5, 7.8 Hz, 6H), 3.59 (s, 3H); ^{13}C NMR (DMSO-d_6, δ in ppm): 192.34, 149.78, 140.41, 132.99, 132.59, 131.98, 129.77, 128.34, 124.54, 118.41, 106.33, 38.01; ^{31}P NMR (DMSO-d_6, δ in ppm): 42.94; IR (cm^{-1}): C═O (1955.77); liquid chromatography–mass spectrometry (LCMS): $[M]^+$ 666.08, [M–Cl + H]—632.10, LCMS: $[PF_6]^-$—144.96, high-resolution mass spectrometry (HRMS) for $[M]^+$ [$C_{32}H_{28}ClN_5OPRu$] Calculated—666.0763, Found—666.0783; Anal. Calcd. For [$C_{32}H_{28}ClN_5OPRu$]Cl: C 59.12, H 4.34, N 10.77 Found: C 59.47, H 4.76, N 11.06.

2.3 | Synthesis of [Ru(CNC)(CO)(PPh_3)Cl]PF_6, 1b

To a solution of **1a** (0.100 g, 0.13 mmol) in 2 ml of methanol, add NH_4PF_6 (0.22 g, 0.13 mmol) and stirred for 30 min at room temperature. A yellow precipitate of **1b** slowly comes out, and on cooling at 0°C, some more precipitation occurred. Yield: 0.035 g (31%). ^{1}H NMR (400 MHz, DMSO-d_6, δ in ppm): δ 8.37 (d, J = 2.4 Hz, 2H), 8.11 (t, J = 8.1 Hz, 1H), 7.72 (d, J = 8.2 Hz, 2H), 7.54 (d, J = 2.2 Hz, 2H), 7.36 (t, 3H), 7.25 (td, J = 7.7, 2.2 Hz, 6H), 6.96 (dd, 6H), 3.61 (s, 3H); ^{13}C NMR (DMSO-d_6, δ in ppm): 192.06, 149.50, 140.49, 132.78, 132.39, 131.93, 129.55, 127.93, 124.52, 118.02, 106.14, 37.82; ^{31}P NMR (DMSO-d_6, δ in ppm): 43.27, 143.87; IR (cm^{-1}): C═O (1954.21); LCMS: $[M]^+$ 666.08, [M–Cl

+ H]—632.11, LCMS: $[PF_6]^-$—144.96, HRMS for $[M]^+$ $[C_{32}H_{28}ClN_5OPRu]$ Calculated—666.0763, Found—666.0807; Anal. Calcd. For $[C_{32}H_{28}ClN_5OPRu]PF_6$: C 47.39, H 3.48, N 8.63 Found: C 47.74, H 3.87, N 8.95.

2.4 | Synthesis of $[Ru(CNC)(PPh_3)_2Cl]Cl$, 2a and $[Ru(CNC)(PPh_3)_2H]cl$, 3a

Similar procedure was followed as with **1a** except $[RuCl_2(PPh_3)_3]$ (0.480 g, 0.5 mmol) was added in place of $[RuHCl(CO)(PPh_3)_3]$. The solvent was reduced in volume (2 ml) followed by the addition of diethyl ether (5 ml) resulting in the precipitation of compound which was filtered and dried under vacuum. Further, the crude solid was purified by column chromatography using neutral alumina with eluting solvent ((hexane/CH_2Cl_2)/CH_3OH) ((1:1):5) gives **3a** and ((hexane/CH_2Cl_2)/CH_3OH) ((1:1):7) affords **2a** as light yellow solids. The X-ray quality crystals of **2a** were obtained by slow diffusion of diethyl ether in acetonitrile solution at −18°C.

Compound **2a**: Yield: 0.155 g (25%). ^{1}H NMR (DMSO-d_6, 500 MHz, δ in ppm): δ 8.31 (d, J = 2.2 Hz, 2H), 7.49 (d, J = 2.1 Hz, 2H), 7.36 (t, J = 7.5 Hz, 1H), 7.29 (t, J = 7.4 Hz, 6H), 7.18–7.12 (m, 12H), 7.06 (d, J = 8.2 Hz, 2H), 7.04–7.00 (m, 12H), 3.59 (s, 3H); ^{13}C NMR (DMSO-d_6, δ in ppm): 188.91, 152.10, 132.92, 132.13, 129.19, 127.69, 125.53, 117.83, 105.22, 48.28, 36.73; ^{31}P NMR (DMSO-d_6, δ in ppm): 31.79, 26.60. LCMS: $[M]^+$ 900.17, $[M–Cl]^{2+}$ 432.59, LCMS: $[M]^-$—144.9636, HRMS for $[M]^+$ $[C_{49}H_{43}ClN_5P_2Ru]$ Calculated—900.1730, Found—900.1714; Anal. Calcd. For $[C_{49}H_{43}ClN_5P_2Ru]Cl$: C 62.89, H 4.63, N 7.48 Found: C 63.14, H 4.89, N 7.72.

Compound **3a**: Yield: 0.058 g (10%). ^{1}H NMR (400 MHz, DMSO-d_6): δ 8.35 (d, J = 2.3 Hz, 2H), 7.84 (t, J = 8.0 Hz, 1H), 7.61 (d, J = 7.9 Hz, 2H), 7.28 (t, J = 7.4 Hz, 6H), 7.25 (d, J = 2.2 Hz, 2H), 7.18 (t, J = 7.6 Hz, 12H), 6.85–6.70 (m, 12H), 2.46 (s, 6H), −8.88 (t, J = 27.0 Hz, 1H); ^{13}C NMR (DMSO-d_6, δ in ppm): 198.09, 149.75, 135.85, 131.66, 128.89, 127.71, 123.92, 117.19, 104.11, 48.43, 35.82; ^{31}P NMR (DMSO-d_6, δ in ppm): 52.10. LCMS: 866.17 $[M]^+$. HRMS for $[M]^+$ $[C_{49}H_{44}N_5P_2Ru]$ Calculated—866.2123, Found—866.2125; Anal. Calcd. For $[C_{49}H_{44}N_5P_2Ru]Cl$: C 65.29, H 4.92, N 7.77 Found: C 65.57, H 5.27, N 8.06.

2.5 | Synthesis of $[Ru(CNC)(PPh_3)_2Cl]PF_6$, 2b

To a solution of **2a** (0.100 g, 0.11 mmol) in 2 ml of methanol, add NH_4PF_6 (0.19 g, 0.11 mmol) and stirred for 30 min at room temperature. A yellow precipitate of **2b** slowly comes out, and on cooling at 0°C, some more precipitation occurred. Yield: 0.034 g (29%).^{1}H NMR (DMSO-d_6, δ in ppm): ^{1}H NMR (500 MHz, DMSO-d_6) δ 8.22 (d, J = 2.2 Hz, 2H), 7.46 (d, J = 2.4 Hz, 2H), 7.36 (t, J = 8.1 Hz, 1H), 7.29 (t, J = 7.5 Hz, 6H), 7.19–7.12 (m, 12H), 7.06–6.99 (m, 12H), 6.98 (d, J = 4.00 Hz, 2H), 3.59 (s, 3H); ^{13}C NMR (DMSO-d_6, δ in ppm): 188.74, 152.09, 132.93, 132.13, 129.18, 127.55, 125.58, 117.75, 105.16, 48.29, 36.72; ^{31}P NMR (DMSO-d_6, δ in ppm): 31.70, 26.57, −144.18. LCMS: $[M]^+$ 900.18, $[M–Cl]^{2+}$ 432.60, LCMS: $[M]^-$—144.96, HRMS for $[M]^+$ $[C_{49}H_{43}ClN_5P_2Ru]$ Calculated—900.1730, Found—900.1739; Anal. Calcd. For $[C_{49}H_{43}ClN_5P_2Ru]PF_6$: C 56.30, H 4.15, N 6.70 Found: C 56.47, H 4.42, N 7.21.

2.6 | Synthesis of $[Ru(CNC)(PPh_3)_2H]Cl$, 3a from 2a

Complex **2a** was added (0.214 mmol, 0.200 g) in a Schlenk tube followed by K_2CO_3 (0.214 mmol, 0.029 g), and then, *i*-PrOH was injected via the syringe. The reaction mixture was refluxed at 85°C for 15 h. The colour of the reaction mixture was changed from greenish-brown to brown orange. After the completion of the reaction, the mixture was filtered, and the solvent was evaporated under a reduced vacuum to afford brown solid. Solid was washed with diethyl ether and dried under vacuum. The complex was obtained with 77.8% yield.

2.7 | Synthesis of $[Ru(CNC)(PPh_3)_2H]PF_6$, 3b

To a solution of **3a** (0.11 mmol, 0.100 g) in methanol, NH_4PF_6 was added and stirred for 30 min at room temperature. A precipitate of **3b** slowly comes out, and on cooling at 0°C, some more precipitation of $[Ru(CNC)(PPh_3)_2(H)]PF_6$ occurred. Yield: 0.060 g (54%). ^{1}H NMR (400 MHz, DMSO-d_6): δ 8.31 (d, J = 4.0 Hz, 2H), 7.85 (t, J = 8.1 Hz, 1H), 7.58 (d, J = 8.5 Hz, 2H), 7.28 (t, J = 7.5 Hz, 6H), 7.24 (d, J = 4.00 Hz 2H), 7.18 (t, J = 7.6 Hz, 12H), 6.90–6.64 (m, 12H), 2.47 (s, 2H), −8.86 (t, J = 27.0 Hz, 1H); ^{13}C NMR (DMSO-d_6, δ in ppm): 201.28, 149.43, 135.54, 131.38, 128.55, 127.41, 123.56, 116.80, 103.74, 47.11, 35.50; ^{31}P NMR (DMSO-d_6, δ in ppm): 51.91, −144.15. LCMS: 866.20 $[M]^+$. HRMS for $[M]^+$ $[C_{49}H_{44}N_5P_2Ru]$ Calculated—866.2123, Found—866.2168; Anal. Calcd. For $[C_{49}H_{44}N_5P_2Ru]PF_6$: C 58.22, H 4.39, N 6.93 Found: C 58.63, H 4.81, N 7.25.

2.8 | X-ray data collection and structure refinement

Single-crystal X-ray data of compounds **1a** and **2a** were collected on Rigaku Oxford Diffractometer using

graphite-monochromated Mo Kα radiation ($\lambda = 0.7107$ Å). The data collection was evaluated with the help of CrysAlisPro CCD software. Data collections for all complexes were carried out at room temperature. Final refinement included atomic positions for all the atoms, anisotropic thermal parameters for all the nonhydrogen atoms and isotropic thermal parameters for all the hydrogen atoms. Full-matrix least-squares refinement against |F2| was carried out using the WinGx package of programs.[30] In **2a**, the disordered lattice chloride ion was refined by splitting them into two parts without fixing any site occupancy factor (sof). The occupancies of the split atoms were refined by means of a free variable. Details of the structural parameters and final refinements for the compounds are given in Table S1.

2.9 | General procedure for catalytic hydrogen transfer reaction

Typically, the ketone (2 mmol) and catalyst (1 mol%) were dissolved in *i*-PrOH (5 ml), under inert atmosphere in two-neck 25-ml R.B. flask equipped with a reflux condenser, followed by addition of Na (1 eq., 2 mmol) to generate *i*-PrONa, in situ. After all the sodium metal had dissolved, the reaction mixture was quickly heated to reflux by lowering into a preheated oil bath. The conversion of the corresponding product at 15-min time intervals was determined by the relative peak area of the substrate and the product in GC without an internal standard (Figures S44–S73). After the reaction was completed, the solution was cooled quickly in an ice bath and analysed by GC–mass spectrometry (MS). The product was purified by silica gel column chromatography using hexane/ethyl acetate (typically 8:2) as eluent to determine the isolated yield. NMR data for alcohol products are given in Figures S74–S81.

3 | RESULTS AND DISCUSSION

3.1 | Synthesis of CNC pincer ruthenium complexes

The imidazolium ligand precursor **CNC·2HBr** was prepared by the reported procedure in literature[31] and characterised by ^{1}H and ^{13}C (Figures S1 and S2). The reaction of imidazolium precursor with Ag_2O, in methanol, affords silver–carbene complex, which undergoes transmetallation with Ru precursors in situ to give Ru–CNC complexes (Scheme 1). When the silver–carbene complex was treated with the [RuHCl(CO)$(PPh_3)_3$] precursor (**Ru1**) for 24 h, **1a** was obtained (Figures S3–S8). Spectroscopic data (^{31}P NMR and LCMS) of the crude reaction mixture indicates that **2a** and **3a** are formed as minor impurity during the synthesis of **1a**. The dissociation of CO ligand and subsequent coordination of PPh_3 ligand, present in the solution, may result in the formation of complex **2a**. The complex **2a**, subsequently, undergoes chloride ligand substitution by a methoxy ligand generated from methanol solvent followed by β-hydride elimination leading to the synthesis of the hydride complex **3a**. Compound **1b** was precipitated out by treating the crude reaction mixture of **1a** with NH_4PF_6 in methanol (Figures S9–S14). The minor impurities from **1a** and **1b** were removed upon precipitation followed by recrystallisation.

A similar reaction condition was used to synthesise **2a** from [$RuCl_2(PPh_3)_3$] as the ruthenium source (**Ru2**). However, the synthesis of compound **2a** is always accompanied by in situ generation of **3a**. Compound **2a** was attempted to purify in the form of **2b**, by precipitation using NH_4PF_6. However, we are unable to separate compound **3b** from **2b**, which also precipitated during the anion exchange. The mixture of complexes **2a** and **3a** can be converted to **3a**, cleanly, as shown in Scheme 2 (vide infra). Spectroscopically pure **2a** was obtained by alumina-gel chromatography followed by recrystallisation (Figures S15–S21). Further, anion exchange of **2a** and **3a** by precipitation using NH_4PF_6 gives **2b** (Figures S22, S23 and S25–S29) and **3b**, respectively.

All the complexes are characterised by IR, mass and multinuclear NMR spectroscopic techniques. In the ^{1}H NMR spectrum (Figure S1), the ligand precursor **CNC·2HBr** exhibits a singlet at $\delta = 10.59$ ppm due to imidazolium proton, and disappearance of this peak indicated the carbene generation during complex formation.

The C═O stretching frequency of 1956 and 1954 cm^{-1} in **1a** and **1b** (Figures S8 and S14), respectively, is significantly larger than 1922 cm^{-1} of Ru–CNC pincer[25] and comparable with previously reported CNC complexes 1952 and 1954 cm^{-1}.[32] Complex **1a** showed signals for ESI^{+} LCMS at *m/z* 632.12 and 666.08 assigned to [**1a**–2Cl + H]$^{+}$ and [**1a**–Cl]$^{+}$, respectively (Figure S6). ^{1}H NMR of **1a** and **1b** are almost identical with the pyridine protons appearing as a doublet at $\delta = 8.44$ and a triplet $\delta = 8.11$ ppm, whereas two doublets are observed at $\delta = 7.77$ and $\delta = 7.56$ for the imidazol-2-ylidene protons (Figures S3 and S9). In the ^{13}C NMR spectra, the carbene carbon signals of **1a** and **1b** appear at 192 ppm (Figures S5 and S11). ^{31}P NMR spectrum of **1a** and **1b** showed peaks at 40.59 and 43.27 ppm (Figures S4 and S10), respectively, for PPh_3 ligand, comparable with previously reported NNN pincer complexes.[33]

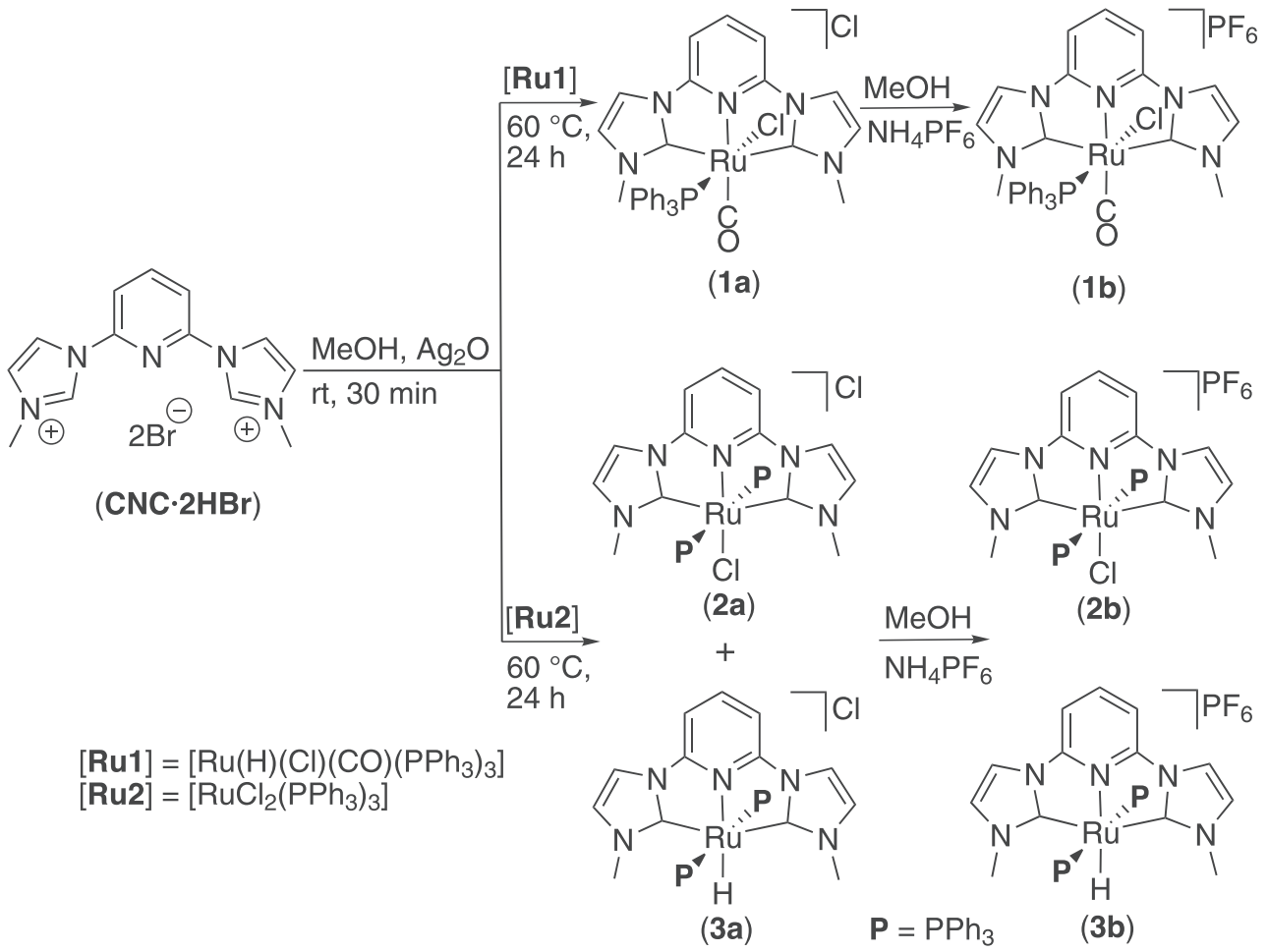

SCHEME 1 Synthesis of CNC pincer ruthenium complexes **1**–**3**

Compounds **2a** and **2b** show ESI^+ LCMS signal at *m/z* 900.00, assigned to $[\mathbf{2a/2b–Cl}]^+$ (Figures S18 and S26). In ^1H NMR of **2a**, one doublet and triplet appear at $\delta = 8.31$ and $\delta = 7.36$ for pyridine protons, whereas imidazol-2-ylidene protons were shown as two doublets at $\delta = 7.49$ and $\delta = 7.06$ (Figure S15). In the case of **2b**, pyridine and imidazolium protons are slightly shifted to downfield than **2a** (Figure S22); however, methyl protons appear at the same value $\delta = 3.59$ ppm for both the complexes (Figures S15 and S22). Interestingly, ^{31}P NMR spectra of complexes **2a** and **2b** show two singlets at 31.79, 26.60, 31.70 and 26.57 ppm (Figures S16 and S23) whereas no dissociation of PPh_3 was observed. The signal at 26.60 ppm was ruled out to be due to $O{=}PPh_3$ by recording the NMR after addition of $O{=}PPh_3$ in the NMR sample of **2a** and **2b** (Figure S24). These complexes are expected to exhibit one singlet in the ^{31}P NMR considering the same chemical environment for the two phosphorus atoms. These two singlets in the ^{31}P NMR are attributed to the generation of two species in solution due to dissociation of the coordinated chloride ligand. This assumption is confirmed by mass analysis where ESI^+ LCMS signal at *m/z* 432.59 is observed and assigned to $[\mathbf{2a–Cl}]^{2+}/[\mathbf{2b–Cl}]^{2+}$ (Figures S19 and S27).

3.2 | Description of the crystal structures

The molecular structures of complexes **1a** and **2a** are confirmed by X-ray crystal diffraction analysis. Complexes **1a** (Figure 1) and **2a** (Figure 2) crystallised in an orthorhombic system with $P2_12_12_1$ space group and monoclinic system with $P21/c$ space group, respectively. The ruthenium metal centre in all the complexes displays distorted octahedral geometry. Selected bond lengths and angles of complexes **1a** and **2a** are listed in Table S2.

Complex **1a** crystallised with bromide ions from the crude reaction mixture whereas the mass data of the purified samples indicated chloride as the halide present in the coordination sphere. The molecular structure of **1a** consists of a six-coordinate Ru(II) centre with

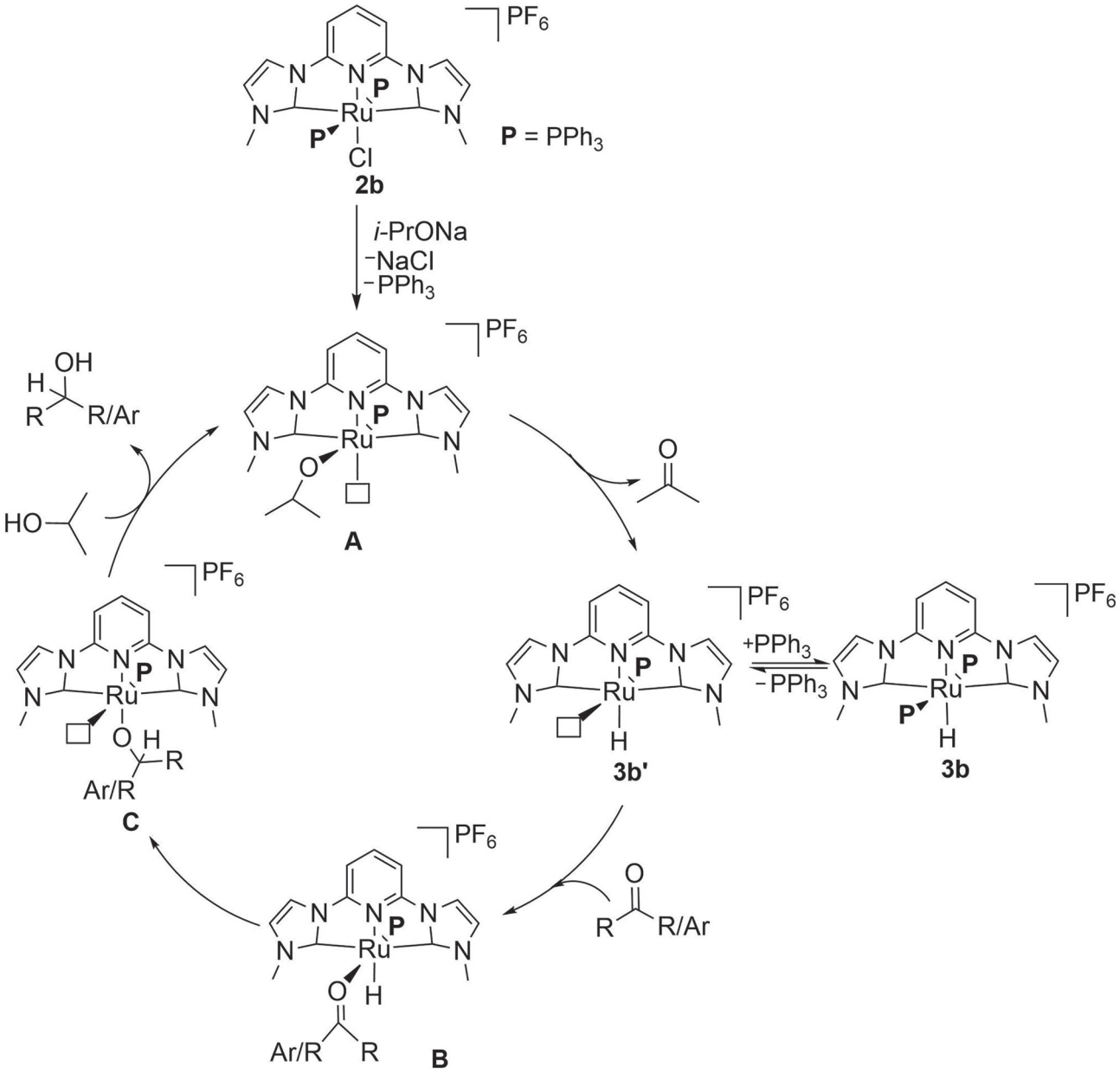

SCHEME 2 Plausible mechanism for transfer hydrogenation catalysis by **2b**

Br^- and triphenylphosphine at the axial positions, CO trans to the pyridine nitrogen atom and CNC pincer ligand at the meridional site (Figure 1). Another bromide ion is present in the lattice. The CNC pincer ligand occupies three meridional sites with C1-Ru1-C10 angle of 152.3(4), shorter than the previously reported complexes.[32] The bite angle (N3-Ru1-C10) of 76.8(4)° is similar to the complex reported by Poyatos et al.[25] The bond distances of Ru1-C1 (2.051(9) Å) and Ru1-C10 (2.085(9) Å) are comparable with the reported ruthenium NHC carbene complexes 2.056(5) and 2.062(5) Å.[25] The CO molecule is present trans to the pyridine ring, and Ru-C (CO) bond length of 1.875(13) Å is equivalent to those reported in the literature.[25,32] The C-O bond length of 1.114(13) Å (Table S2) is comparable with NNN pincer (C-O, 1.105(6) Å)[33] complex and slightly shorter than the previously reported CNC complex (C-O, 1.152 (6) Å).[25]

Complex **2a** also has distorted octahedral geometry in which Ru(II) is surrounded by one CNC pincer ligand, two triphenylphosphines and one chloride ion (Figure 2). The two bulky triphenylphosphines are situated trans to each other. The N3-Ru1-C10 bite angle is 77.5(3)° and comparable with the previously reported complexes.[25] The bond distance of Ru1-C1 (2.052 (6) Å) (Table S2) is similar to that in the complex **1a** and comparable with the reported complex[25] (2.056(5) Å) distance whereas Ru1-C10 (2.094(7) Å) was slightly larger than the

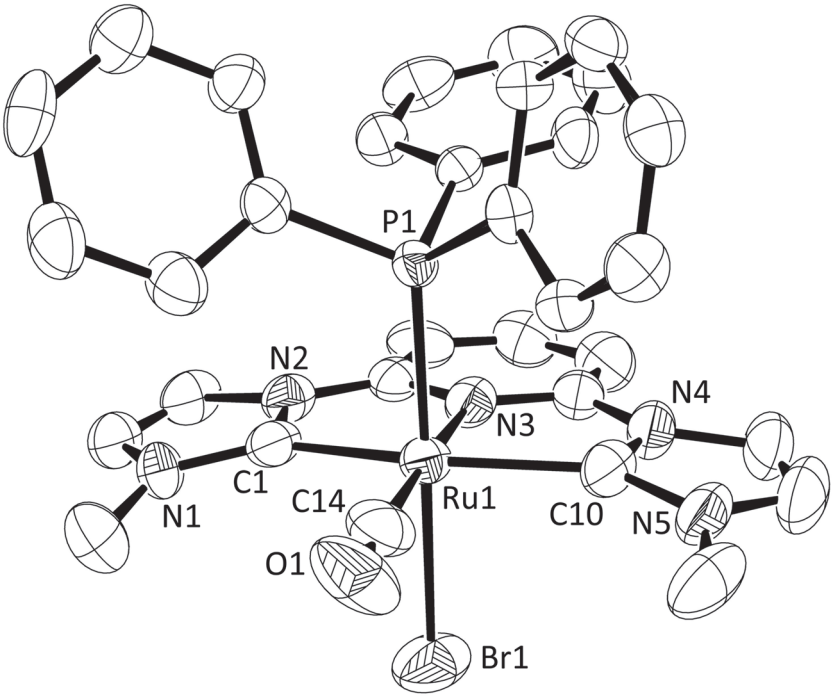

FIGURE 1 Molecular structure of **1a** with thermal ellipsoids drawn at the 50% level. All hydrogen atoms and a bromide counterion are omitted for clarity. Selected bond lengths (Å) and angles (°): Ru1-N3, 2.077(8), Ru1-C1, 2.051 (9); Ru1-C10, 2.085(9); Ru1-C14, 1.875(13); Ru1-P1, 2.342(2); Ru1-Br1, 2.5727(13); C1-Ru1-C10, 152.3(4); N3-Ru1-C10, 76.8(4); N3-Ru1-P1, 90.7(2); C10-Ru1-P1, 94.8(3); C1-Ru1-Br1, 85.6(2); N3-Ru1-Br1, 87.2(2); C10-Ru1-Br1, 86.6(3); P1-Ru1-Br1, 177.20(6)

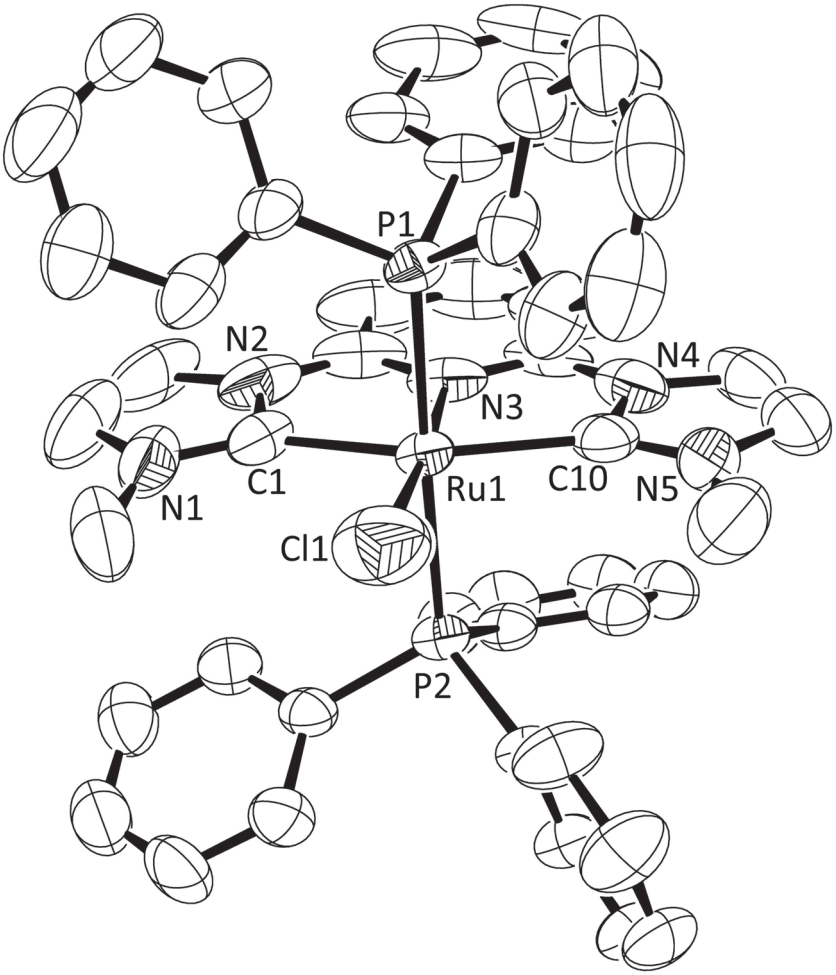

FIGURE 2 Molecular structure of **2a** with thermal ellipsoids drawn at the 50% level. All hydrogen atoms and a chloride counterion are omitted for clarity. Selected bond lengths (Å) and angles (°): Ru1-N3, 2.020(5), Ru1-C1, 2.052 (6); Ru1-C10, 2.094(7); Ru1-P1, 2.370(1); Ru1-P2, 2.359(1); Ru1-Cl1, 2.447(3); C1-Ru1-C10, 156.1 (3); N3-Ru1-C10, 77.5(3); N3-Ru1-P1, 90.76(13); C10-Ru1-P1, 89.68(15); C1-Ru1-Cl1, 97.80(19); N3-Ru1-Cl1, 176.05(18); C10-Ru1-Br1, 106.1(2); P1-Ru1-Cl1, 87.73(7); P2-Ru1-Cl1, 89.12(7)

complex **1a** and the previously reported complex (2.062 (5) Å).[25] The Ru-P (Ru1-P1, 2.370(1)Å and Ru1-P2, 2.359(1) Å) bonds in case of **2a** are slightly longer than the **1a** (Ru1-P1, 2.342 (2) Å) and previously reported complex (Ru1-P1, 2.318(2) Å).[24]

3.3 | Catalytic application in TH

Ruthenium complexes **1b**, **2b** and **3b** were used as catalyst for TH of ketones using 2-propanol, and the reaction was monitored by GC without internal standard. Initially, the TH of cyclohexanone in refluxing 2-propanol was selected as a model reaction to evaluate the catalytic activity of complexes. Using 2 mmol of ketone, 1 mol% of catalyst and 1 equivalent of sodium isopropoxide (*i*-PrONa) as base complex **1b** showed higher catalytic activity than other complexes, namely, **2b** and **3b**, resulting in >99% conversion of cyclohexanone in 30 min (Table 1, Entry 2). Under similar conditions, complexes **2b** and **3b** exhibited slightly lower catalytic activity with 61% and 72% conversion (Table 1, Entries 3 and 4). Further, the effect of various bases, for example, NaOH, KOH and KO^{t}Bu, in different time intervals (15 and 30 min) with complex **1b** was also studied (Table 1, Entries 5–10). The conversion of cyclohexanone to corresponding alcohol was achieved in 79%, 74% and 78% in 30 min (Table 1, Entries 6, 8 and 10) and 55%, 71% and 0% in 15 min (Table 1, Entries 5, 7 and 9) using the bases NaOH, KOH and KO^{t}Bu, respectively, indicating there is a significant induction period for catalysis with KO^{t}Bu. As the results, ruthenium complex **1b** (1 mol%) as catalyst and *i*-PrONa as base in isopropanol under reflux temperature were chosen as suitable reaction condition.

The scope of the catalyst **1b** was then examined using various ketone substrates to establish the generality of the reaction. Several ketone derivatives with aliphatic and aromatic substituents, as well as both the electron-donating and electron-withdrawing substituents, were investigated (Table 2). Aliphatic cyclic ketones (Table 2, Entries 1 and 3) gave good to moderate conversions in 30 min and 1 h, However, the reaction proceeds comparatively slowly in case of aliphatic acyclic ketone (Table 2, Entry 2). For aromatic ketones, the yield varies from 58% to 99% in 1 h (Table 2, Entries 4–10). The electron-withdrawing substituents like Br at the *para* position (Table 2, Entry 5) showed comparable conversion with acetophenone, but in case of chloro (Table 2, Entry 5), reactivity of reaction was slightly decreased. Subsequently, the electron-donating methyl substituents

TABLE 1 Optimisation table of different catalysts

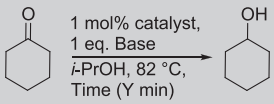

Entry[a]	Catalyst	Base	Time (min)	Conversion[b] (%)	TON/TOF (h^{-1})
1	**1b**	*i*-PrONa	15	85	85/340
2	**1b**	*i*-PrONa	30	>99	99/198
3	**2b**	*i*-PrONa	30	61	61/122
4	**3b**	*i*-PrONa	30	72	72/144
5	**1b**	NaOH	15	55	55/220
6	**1b**	NaOH	30	79	79/158
7	**1b**	KOH	15	71	71/284
8	**1b**	KOH	30	74	74/148
9	**1b**	KO^{t}Bu	15	0	-
10	**1b**	KO^{t}Bu	30	78	78/156
11	**1b**	*i*-PrONa	15	48[c]	96/384
12	**1b**	*i*-PrONa	30	51[c]	102/204

Note: TON = (Number of moles of substrate converted)/(Number of moles of catalyst), at the end of the reaction. TOF = [(TON)/h].

[a]Reaction conditions: ketone (2.0 mmol), catalyst ([**Ru**] 1 mol%), *i*-PrONa (1 eq.), *i*-PrOH (5 ml), at 82°C under a slow N_2 flow.

[b]Determined by gas chromatography without internal standard.

[c]Catalyst ([**Ru**] 0.5 mol%).

TABLE 2 Transfer hydrogenation of various ketones with catalyst **1b**

Entry[a]	Reactant	Product	% Conversion[b] (isolated yield) 0.5 h	1 h	TON/TOF (h^{-1})
1		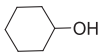	>99 (98)	-	98/196
2	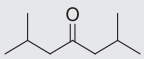	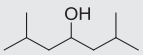	24	37 (30)	30/30
3		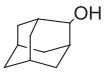	65	80 (62)	62/62
4		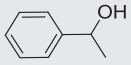	80	>99 (95)	95/95
5	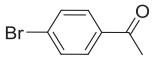	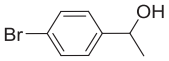	60	97 (75)	75/75
6	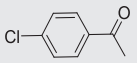	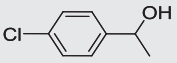	58	84 (80)	80/80
7	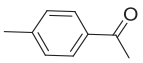	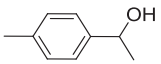	32	58 (45)	45/45
8	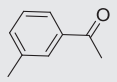	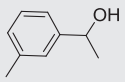	24	68 (53)	53/53
9	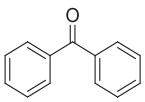	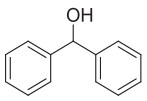	12	73 (67)	67/67
10	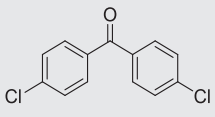	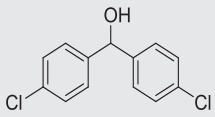	70	83 (64)	64/64

Note: TON = (Number of moles of substrate converted)/(Number of moles of catalyst), at the end of the reaction. TOF = [(TON)/h].

[a]Reaction conditions: ketone (2.0 mmol), **1b** ([Ru] 1 mol%), *i*-PrONa (1 eq.), *i*-PrOH (5 ml), at 82°C under a slow N_2 flow for 1 h.

[b]Determined by gas chromatography without internal standard.

at *para* and *meta* positions (Table 2, Entries 7 and 8) relatively decelerated the rate of TH. Benzophenone was reduced in 1 h with 73% conversion, whereas 4,4′-dichlorobenzophene gave 83% conversion (Table 2, Entries 9 and 10). For the unexpected high reactivity of benzophenone, we believe that after the dissociation of one PPh_3 ligand, the steric environment around Ru centre is not so crowded to prevent its coordination to the Ru. Further, the bulkiness of the product may be helpful in the dissociation from the catalyst which can,

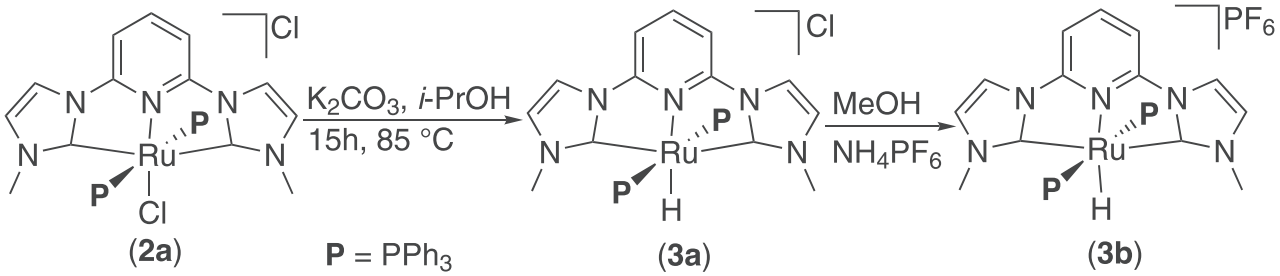

SCHEME 3 Synthesis of CNC pincer ruthenium complexes **3a** and **3b** from **2a**

then, start another catalytic cycle. The alcohols were isolated in good to excellent yield after column chromatography as reported in Table 2.

A plausible mechanism for transfer hydrogenation is shown in Scheme 3, with complex **2b** as the catalyst precursor and **3b** as the Ru-hydride intermediate. A similar mechanism may also be suggested to be operating during the catalysis with **1b**. It is worth mentioning that the corresponding Ru-hydride species for **1b** is observed in the fragmentation pattern of **1a** in LCMS as [**1a**–2Cl + H]$^+$; however, attempts to synthesise or identify this Ru-hydride intermediate under catalytic conditions have been unsuccessful, probably due to its high reactivity. Therefore, mechanistic studies were performed on catalysis with complexes **2b** and **3b**. ^{31}P NMR of an NMR scale experiment with 1 equivalent each of **2b**, base and 2-propanol indicates the presence of free PPh_3 ligand and the generation of the hydride complex **3b** in the catalytic reaction mixture (Figure S43). A sample of the reaction mixture during catalysis was taken for LCMS mass analysis. Analysis of the mass data of the reaction mixture during catalysis indicates the presence of hydride complex **3b** supporting the proposed mechanism (Figure S42).

Based on the ^{31}P NMR and mass analyses of the catalytic samples, it is proposed that in the presence of *i*-PrONa, complex **2b** generates the ruthenium alkoxide species **A**. The Ru–H intermediate **3b′** is formed from **A** via β-H elimination by releasing one molecule of acetone or by dissociation of a PPh_3 ligand if starting from **3b**. Addition of a ketone to the intermediate **3b′** produces another ruthenium alkoxide intermediate **B**, which releases the hydrogenated product upon protonation from *i*-PrOH resulting in the formation of **A** again.

To further confirm our proposed mechanism, we have synthesised **3b** from **2a** and performed a catalytic test run starting from **3b**. The reaction of complex **3a** with K_2CO_3 in refluxing *i*-PrOH for 15 h affords clean synthesis of hydride intermediate complex **3a** (Scheme 3).

The pure hydride complex **3a** was characterised by ^{1}H, ^{13}C, IR and MS (Figures S30–S32, S34 and S35). ESI$^+$ LCMS of **3a** displayed signal at *m/z* 866.2 assigned to [**3a**]$^+$ (Figure S33), matching with the catalytic sample mass. Anion exchange of complex **3a** with NH_4PF_6 was carried out to obtain the cleaner data of **3b** (Figures S36–S41). In ^{1}H NMR of **3b**, the hydrido signal gives a triplet at $\delta = -8.86$ ppm, which is indicative of Ru–H complex with two phosphines (Figure S36). Similarly, signals assignable to the pyridine protons and imidazol-2-ylidene protons appeared at $\delta = 8.31$ as a doublet, $\delta = 7.85$ ppm as triplet and two doublets at $\delta = 7.58$ ppm and $\delta = 7.24$ ppm (Figure S36). All the aromatic protons are slightly shifted to downfield in comparison to **2a**, though methyl protons show significant upfield shift at $\delta = 2.47$ ppm. ^{31}P NMR spectrum of **3b** showed peaks at $\delta = 51.96$ for PPh_3 and $\delta = 144.16$ ppm for PF_6, respectively (Figure S37).

4 | CONCLUSIONS

In summary, we have investigated the synthesis and characterisation of ruthenium pincer complexes [Ru(CNC)(CO)(PPh_3)Cl]X (X = Cl^- [**1a**], PF_6^- [**1b**]), [Ru(CNC)(PPh_3)$_2$Cl]X (X = Cl^- [**2a**], PF_6^- [**2b**]) and [Ru(CNC)(PPh_3)$_2$(H)]X (X = Cl^- [**3a**], PF_6^- [**3b**]) containing a 'pyridine–dicarbene' pincer ligand. All the ruthenium complexes were found catalytically active for the transfer hydrogenation of ketones using propan-2-ol. The in situ transformations of these complexes during their synthesis were also observed, which helps in understanding their behaviour during transfer hydrogenation catalysis. Complex **1b** was found to be more active for these transformations than **2b** and **3b** under the optimised conditions. Subsequently, the substrate scope for transfer hydrogenation catalysis with a range of substituted ketones was studied with complex **1b** as the catalyst precursor. Further investigations with lower catalyst loadings while increasing the reaction time and applications of these complexes in related catalyses like acceptorless alcohol oxidation and *N*-alkylation of amines are currently undergoing.

ACKNOWLEDGEMENTS

A.K.S. acknowledges Science and Engineering Research Board, Department of Science and Technology, Government of India for funding this study (EMR/2016/004076). The authors are grateful to the Sophisticated Instrumentation Centre (SIC), IIT Indore, for single-crystal X-ray diffraction and other characterisation facilities.

AUTHOR CONTRIBUTIONS

Dibya Yadav: Data curation; formal analysis; investigation; methodology. **Shilpi Misra:** Formal analysis; investigation; methodology. **Dheeraj Kumar:** Data curation; formal analysis. **Suryabhan Singh:** Data curation; methodology. **Amrendra Singh:** Conceptualization; funding acquisition; project administration; supervision.

CONFLICT OF INTEREST

There are no conflicts of interest to declare.

DATA AVAILABILITY STATEMENT

Additional data that support the findings of this study are available in the supplementary material of this article.

ORCID

Dibya Yadav https://orcid.org/0000-0001-7310-6883
Shilpi Misra https://orcid.org/0000-0002-2408-841X
Dheeraj Kumar https://orcid.org/0000-0002-7259-937X
Suryabhan Singh https://orcid.org/0000-0002-9078-6240
Amrendra K. Singh https://orcid.org/0000-0001-7263-7914

REFERENCES

[1] C. Gunanathan, D. Milstein, *Chem. Rev.* **2014**, *114*, 12024.
[2] S. Murugesan, K. Kirchner, *Dalton Trans.* **2016**, *45*, 416.
[3] R. E. Andrew, L. Gonzalez-Sebastian, A. B. Chaplin, *Dalton Trans.* **2016**, *45*, 1299.
[4] Y. Arikawa, T. Nakamura, T. Higashi, S. Horiuchi, E. Sakuda, K. Umakoshi, *Eur. J. Inorg. Chem.* **2017**, 881.
[5] G. van Koten, D. Milstein (Eds), *Organometallic Pincer Chemistry*, Topics in Organometallic Chemistry Vol. 40, Springer **2013**.
[6] K. J. Szabo, O. F. Wemdt, *Pincer and Pincer-Type Complexes: Applications in Organic synthesis and Catalysis*, Wiley-VCH **2014**.
[7] a) J. I. vander Vlugt, J. N. H. Reek, *Angew. Chem., Int. Ed.* **2009**, *49*, 8832. b) J. I. vander Vlugt, J. N. H. Reek, *Angew. Chem.* **2009**, *121*, 8990.
[8] J. Choi, A. H. R. MacArthur, M. Brookhart, A. S. Goldman, *Chem. Rev.* **2011**, *111*, 1761.
[9] H. A. Younus, W. Su, N. Ahmad, S. Chen, F. Verpoort, *Adv. Synth. Catal.* **2015**, *357*, 283.
[10] R. R. Schrock, *Nat. Chem.* **2011**, *3*, 95.
[11] K. Arashiba, Y. Mikyake, Y. Nishibayashi, *Nat. Chem.* **2011**, *3*, 120.
[12] S. Kuriyama, K. Arashiba, K. Nakajma, H. Tanaka, K. Yoshizawa, Y. Nishibayashi, *Eur. J. Inorg. Chem.* **2016**, *30*, 2856.
[13] M. J. Bezdek, S. Guo, P. J. Chirik, *Inorg. Chem.* **2016**, *55*, 3117.
[14] J. Zhao, A. S. Goldman, J. F. Hartwig, *Science* **2005**, *307*(5712), 1080.
[15] M. J. Bezdek, S. Guo, P. J. Chirik, *Science* **2016**, *354*, 730.
[16] Z. Chen, J. J. Concepcion, M. K. Brennaman, P. Kang, M. R. Norris, P. G. Hoertz, T. J. Meyer, *Proc. Natl. Acad. Sci. U. S. A.* **2012**, *109*, 15606.
[17] A. Genoni, D. N. Chirdon, M. Boniolo, A. Sartorel, S. Bernhard, M. Bonchio, *ACS Catal.* **2017**, *7*, 154.
[18] K. Tanaka, H. Isobe, S. Yamanaka, K. Yamaguchi, *Proc. Natl. Acad. Sci. U. S. A.* **2012**, *109*, 15600.
[19] X. Lin, X. Hu, J. J. Concepcion, Z. Chen, S. Liu, T. J. Meyer, W. Yang, *Proc. Natl. Acad. Sci. U. S. A.* **2012**, *109*, 15669.
[20] M. D. Kärkäs, O. Verho, E. V. Johnston, B. Åkermark, *Chem. Rev.* **2014**, *114*, 11863.
[21] J. D. Blakemore, R. H. Crabtree, G. W. Brudvig, *Chem. Rev.* **2015**, *115*, 12974.
[22] J. Creus, R. Matheu, I. Peñafiel, D. Moonshiram, P. Blondeau, J. Benet-Buchholz, J. García-Antón, X. Sala, C. Godard, A. Llobet, *Angew. Chem., Int. Ed.* **2016**, *55*, 15382.
[23] V. Charra, P. de Frémont, P. Braunstein, *Coord. Chem. Rev.* **2017**, *341*, 153.
[24] A. A. Danopoulos, S. Winston, W. B. Motherwell, *Chem. Commun.* **2002**, 1376.
[25] M. Poyatos, J. A. Mata, E. Falomir, R. H. Crabtree, E. Peris, *Organometallics* **2003**, *22*, 1110.
[26] N. Meyer, A. J. Lough, R. H. Morris, *Chem. – Eur. J.* **2009**, *15*, 5605.
[27] A. Gavriilidis, A. Constantinou, K. Hellgardt, K. K. Hii, G. J. Hutchings, G. L. Brett, S. Kuhn, S. P. Marsden, *React. Chem. Eng.* **2016**, *1*, 595.
[28] N. Ahmad, J. J. Lavison, S. D. Robinson, M. F. Uttley, *Inorg. Synth. 15*, 48.
[29] P. S. Hallman, T. A. Stephenson, G. Wilkinson, *Inorg. Synth. 12*, 238.
[30] L. J. Farrugia, *J. Appl. Crystallogr.* **2012**, *45*, 849.
[31] D. J. Nielsen, K. J. Cavell, B. W. Skelton, A. H. White, *Inorg. Chim. Acta* **2006**, *359*, 1855.
[32] X. W. Li, F. Chen, W. F. Xu, Y. Z. Li, X. T. Chen, Z. L. Xue, *Inorg. Chem. Comm.* **2011**, *14*, 1673.
[33] B. Zhang, H. Wang, X. Yan, Y. A. Duan, S. Guo, F. X. Luo, *Transition Met. Chem.* **2020**, *45*, 99.

SUPPORTING INFORMATION

Additional supporting information may be found online in the Supporting Information section at the end of this article.

How to cite this article: D. Yadav, S. Misra, D. Kumar, S. Singh, A. K. Singh, *Appl Organomet Chem* **2021**, e6287. https://doi.org/10.1002/aoc.6287